HHS Public Access

Author manuscript

Mitochondrion. Author manuscript; available in PMC 2023 May 01.

Published in final edited form as:

Mitochondrion. 2022 May ; 64: 19–26. doi:10.1016/j.mito.2022.02.005.

Cancer/Testis Antigen 55 is required for cancer cell proliferation and mitochondrial DNA maintenance

Jade Aurrière[1], **David Goudenege**[2], **Simone A Baechler**[3], **Shar-Yin N Huang**[3], **Naig Gueguen**[2], **Valerie Desquiret-Dumas**[2], **Floris Chabrun**[2], **Rodolphe Perrot**[4], **Arnaud Chevrollier**[1], **Majida Charif**[1], **Olivier Baris**[1], **Yves Pommier**[3], **Guy Lenaers**[1], **Salim Khiati**[1,*]

[1] MitoLab Team, MitoVasc Unit, CNRS UMR6015, INSERM U1083, SFR ICAT, Angers University, Angers, France.

[2] MitoLab Team, Institut MitoVasc, CNRS UMR6015, INSERM U1083, Angers University, Angers, France; Departments of Biochemistry and Genetics, University Hospital Angers, Angers, France.

[3] Laboratory of Molecular Pharmacology, Developmental Therapeutics Branch, Center for Cancer Research, National Cancer Institute, NIH, Bethesda, MD, USA

[4] SCIAM, Institut de Biologie en Sante, Angers University, Angers 49933, France.

Abstract

Cancer/Testis Antigens (CTAs) represent a group of proteins whose expression under physiological conditions is restricted to testis but activated in many human cancers. Also, it was observed that co-expression of multiple CTAs worsens the patient prognosis. Five CTAs were reported acting in mitochondria and we recently reported 147 transcripts encoded by 67 CTAs encoding for proteins potentially targeted to mitochondria. Among them, we identified the two isoforms encoded by CT55 for whom the function is poorly understood. First, we found that patients with tumors expressing wild-type CT55 are associated with poor survival. Moreover, CT55 silencing decreases dramatically cell proliferation. Second, to investigate the role of CT55 on mitochondria, we first show that CT55 is localized to both mitochondria and endoplasmic reticulum (ER) due to the presence of an ambiguous N-terminal targeting signal. Then, we show that CT55 silencing decreases mtDNA copy number and delays mtDNA recovery after an acute depletion. Moreover, demethylation of CT55 promotor increases its expression, which in turn increases mtDNA copy number. Finally, we measured the mtDNA copy number in NCI-60 cell lines and screened for genes whose expression is strongly correlated to mtDNA amount. We identified *CT55* as the second highest correlated hit. Also, we show that compared to siRNA scrambled control (siCtrl) treatment, CT55 specific siRNA (siCT55) treatment down-regulates

* Corresponding author: Salim KHIATI. MitoLab team, Mitochondrial Medicine Research Centre, Unité MitoVasc, Université d'Angers, UMR CNRS 6015, INSERM U1083, CHU Bât IRIS/IBS, Rue des Capucins, 49933 Angers cedex 9, FRANCE. salim.khiati@univ-angers.fr, Tel : 33/0 244 68 84 05 Fax: 33/0 244 68 65 94.

Declaration of Competing Interest

The authors declare that they have no known competing financial interests or personal relationships that could have appeared to influence the work reported in this paper.

aerobic respiration, indicating that CT55 sustains mitochondrial respiration. Altogether, these data show for first time that CT55 acts on mtDNA copy number, modulates mitochondrial activity to sustain cancer cell proliferation.

Keywords

CT55; mitochondrial DNA; cell proliferation; NCI-60

1. Introduction

Cancer/Testis Antigens (CTAs) constitute one of the most interesting class of tumour-associated antigens and many of them are promising vaccine candidates. Indeed, they are immunogenic proteins expressed only in testis and in various types of cancers. The first Cancer/Testis Antigen, MAGE-A1, was cloned from the cells of a melanoma patient on 1991[1], and as of today, 276 CTAs have been identified and compiled in a unique CTA-Database (http://www.cta.lncc.br/)[2]. Most CTAs are broadly expressed during metastasis, while less frequently in primary tumors. Also, it was observed that co-expression of multiple CTAs at later stages of cancer worsens the prognosis. For instance, multiple myeloma patients expressing more than 6 CTAs have a poorer prognosis than those expressing less than 6 CTAs[3]. Interestingly, five CTAs were reported acting on mitochondria, including COX6B2, FATE1, which are well characterized, SPATA19, GPAT2, and KIAA0100, for whom more investigations are needed to well understand their functions. On one hand, COX6B2 (Cytochrome c Oxidase VIb-2), is a testis specific subunit of the complex IV of the mitochondrial electron transport chain[4] and reported in two cancer models sustaining mitochondrial activities[5,6]. On the other hand, FATE1 disrupts the ER/mitochondrial contacts, in order to prevent Ca^{2+} uptake by mitochondria, thus leading to an inhibition of Ca^{2+}-dependent apoptosis [7]. Also, FATE1 inhibits a pro-apoptotic pathway, by preventing BIK (BCL2-Interacting Killer) accumulation to promoting cell survival[8]. Additionally to these CTAs, we recently reported 143 transcripts encoded by 67 CTAs genes, with a potential mitochondrial targeting sequence (MTS), that we called mitoCTAs [9]. The vast majority of these mitoCTAs have almost no known function in mitochondria.

CT55, also known as BJ-HCC-20 and CXorf48, was among the mitoCTAs with high MTS prediction score. This gene was firstly discovered by analyzing the potential coding sequences of the q26–28 region of human X chromosome. It was identified as CTA because its expression was observed in several tumors and only in testis in physiological conditions [10]. CT55 code for two protein isoforms, a long isoform with 264 amino acids (aa) and a short isoform with 242 aa, lacking the 22 aa residues at the C-terminus. The analysis of the expression of the CTAs in 89 patient tissues with head and neck squamous cell carcinoma revealed that CT55 is usually co-expressed with other CTAs, such as SPANX-CD, MAGEB2, MAGEA1 and MAGEB6, and its expression is related to a poor prognosis [11].

It was reported that CT55 could be a valid therapeutic target for immunotherapy in treatment-free remission of chronic myeloid leukemia patients [12]. Indeed, the authors

reported that the cytotoxic T cells induced with the 49–57aa peptide from CT55 protein sequence recognize and lyse the CIR-A24 cells pulsed with this peptide. Although, the expression of CT55 in several cancer is well known, its function is still poorly understood. Recently, Zhao *et al*, reported that CT55 expression increases inflammatory responses in colitis-associated cancer and tumorigenesis in an azoxymethane/dextran sulfate sodium mouse model[13]. However, its role in mitochondria has never been investigated.

Given the fact that mitochondria play a critical role in cancer [14], and that expression of CT55 is related to poor prognosis, we hypothesize that its function in mitochondria might be essential for cancer cells. To approach this, we analyzed CT55 expression pattern in relation to patient prognosis for several types of cancers, and we investigated its potential roles in cell proliferation and mitochondria.

2. Materials and methods

2.1 Cell culture and siRNAs transfection

UACC-62, SK-MEL-2, HCT-116 and SNB-75 cells were obtained from NCI (National Cancer Institute) and cultured in standard growth medium (Dulbecco's modified Eagle's medium (DMEM); Gibco) supplemented with 10% fetal bovine serum (FBS; PAN Biotech), 1mM of sodium pyruvate (Gibco) and 1mM L-glutamine (Dutscher) at 37 °C in presence of 5% CO2. For CT55 silencing, UACC-62 cells were transfected with 5 nM CT55 specific siRNA (siCT55) (SR310386; Origene) or scrambled control (siCtrl), using Lipofectamine RNAiMAX (Invitrogen) according to the manufacturer's specifications. Silencing efficiency was tested by RTqPCR and Western blot analysis, 72 h after transfection.

2.2 RT-qPCR analysis

UACC62 cells were seeded at the density of 50.000 cells/well in 6-well plates for 24 hours then transfected with SiRNA. After 3 days of transfection, cells were harvested and suspended in 100 µl phosphate-buffered saline (PBS), and total RNA was purified by using an RNeasy Mini Kit (Qiagen, Cat.#74104) according to the manufacturer's protocol. 1 µg of RNA was reverse transcribed using Invitrogen™ SuperScript™ II Reverse Transcriptase (ThermoFisher, Cat.# 18064071) and qPCRs were performed in triplicate in 384-well reaction plates (Applied Biosystems). Each reaction (final volume 10 µl) contained 10 ng of cDNA, 5 µl of Power SYBR-Green PCR Master Mix (Applied Biosystems) and 0.5 µM of each forward and reverse primer. Two set of primers were used to quantify CT55 and nuclear β2 microglobulin (B2M) was used as housekeeping gene. Primers sequences are in the table below.

	Forward	**Reverse**
B2M	CAGCAAGGACTGGTCTTTCTATCTC	TCTCGATCCCACTTAACTATCTTGGG
CT55–1	CCCTCAGACTCAGGAACCAGAGT	AGATGCCTGGCTCAGTGGAATATTC
CT55–2	CTCTCCACCATGACCACATTGACG	CTGTGAAGCCCATCCGTTGTATTC
TOP2A	ACCCAGCAAATGTGGGTTTAC	CCGGATCAATTGTGACTCTAATAC

	Forward	Reverse
MKi67	TCCATGAGCAGGAGGCAATATTAC	CATTTTCATACCTGAAGGAACGATC
PCNA	GTGAACCTCACCAGTATGTCC	TCTGAAACTTTCTCCTGGTTTGG

2.3 Quantification of mtDNA copy number

Total DNA was isolated from cells using DNeasy Blood and Tissues Kit (Qiagen) according to the manufacturer's specifications. qPCRs were performed in triplicate in 96-wells or 384-wells reaction plates (Applied Biosystems). Each reaction (final volume 10 µl) contained 20 ng DNA, 5 µl of Power SYBR-Green PCR Master Mix (Applied Biosystems) and 0.5 µM of each forward and reverse primer. Mitochondrial ND1 gene was amplified together with the nuclear β2 microglobulin (B2M) gene, as a normalizing control. Primer sequences are:

ND1-F	AAGTCACCCTAGCCATCATTCTAC
ND1-R	GCAGGAGTAATCAGAGGTGTTCTT
β2m-F	TGCTGTCTCCATGTTTGATGTATCT
β2m-R	TCTCTGCTCCCCACCTCTAAGT

2.4 CT55 constructs

Two plasmids pEGFP-N1 (Addgene, #6085–1) and pCMV6-XL5-CT55 (Origene, #SC122337) were used to amplify and clone all the sequences encoding the different CT55 constructs at the EcoR1 and ApaI restriction sites of the pEGFP-N1vector, in fusion with the eGFP. The amplification of the fragments was made by PCR using CloneAmp™ HiFi PCR premix (Takara Bio, Cat#639298). The PCR products were inserted at the EcoR1 and ApaI restriction sites of the pEGFP-N1vector (Addgene, #6085–1) using In-Fusion HD Cloning Plus Kits (Takara Bio, Cat.# 638910) according to the manufacturer's protocol. To clone the N-terminal 12 aa, double strand DNA 5'-CTCAAGCTTCGAATTATGCTCAGGCTTCTGAGACTTGCTTTGGCCTTCTACCGGGATCCACCGGTC-3' was synthesized by Thermo Fisher Scientific and cloned in pEGFP-N1.

Primer sequences used to clone others constructs are :

CT55 constructs	Primers	Primers sequences 5'-3'
CT55-GFP	Forward	CTCAAGCTTCGAATTATGCTCAGGCTTCTGAGACTTGC
	Reverse	GACCGGTGGATCCCGAATGCTTTGGCTCCGACGTTC
N-terminal 30 aa	Forward	CTCAAGCTTCGAATTATGCTCAGGCTTCTGAGACTTGC
	Reverse	GACCGGTGGATCCCGTGGGAGGCCCTGCTGCTG
CT55A30aa	Forward	CTCAAGCTTCGAATTATGCAAGGTGACACCCAGTTGACAAC
	Reverse	GACCGGTGGATCCCGAATGCTTTGGCTCCGACGTTC

2.5 Live-cell confocal imaging

UACC-62 cells were transfected with plasmids encoding different constructs, and when required with plasmids encoding DsRed2-ER-5 (Addgene, #55836) and seeded at the density of 5,000 cells/well in four-well glass-bottom µ-slides (Ibidi, #80427). After 24h, mitochondria were stained using MitoTracker Red (Molecular Probes) at 50 nM, 15 min before confocal live cell imaging. All images were captured using a Leica TCS SP8 confocal microscope with a 40×1.20 NA water objective lens (Leica Microsystems) equipped with a GaAsP Hybrid detector (HyD), at 37°C. On average, 10 image planes were recorded.

2.6 Western-blot

Protein lysates were prepared using RIPA buffer (Thermo Scientific™) supplemented with 1X protease inhibitor cocktail (Roche). After centrifugation at 15 000g for 15 mn, 40 µg of protein in supernatant were subjected to SDS-PAGE and transferred onto PVDF membranes (Amersham Hybond 0.45 µm PVDF). Membranes were blocked for 1h with 5% milk in Tris-Buffered Saline with 0.1% Tween 20 (TBST), then incubated overnight with the following primary antibodies at 1:5000 dilution: mouse polyclonal CT55 (CXorf48) antibody (Abcam, ab69317), alpha Tubulin antibody (Abcam, ab7291). After washing in TBST, membranes were incubated with horseradish peroxidase (HRP)-conjugated goat anti-mouse-IgG or anti-rabbit-IgG (1:10000 dilution) (GE Healthcare) for 1h and washed with TBST. Bands on immunoblots were detected by using SuperSignal West Femto Maximum Sensitivity Substrate (11859290, Pierce).

2.7 mtDNA recovery after ethidium bromide-mediated depletion

50 000 UACC-62 cells were seeded in 6-well plates. After 24 h, cells were switched to medium with 200 nM ethidium bromide and grown for 2 days. After 2 rinses with media, cells were incubated in medium without ethidium bromide and transfected with 5 nM CT55 specific siRNA (siCT55) (SR310386; Origene) or scrambled control (siCtrl), using Lipofectamine RNAiMAX (Invitrogen) according to the manufacturer's specifications. MtDNA was quantified after 2, 3 and 5 days of recovery.

2.8 DNA demethylation

HCT116 cells were seeded at the density of 100.000 cells/well in 6-well plates for 24 hours then treated with 2.5 µM and 5 µM of 5-Aza-2′-deoxycytidine (Sigma, Ref.A3656–5MG). After 3 days of treatment, RNA was harvested and subjected to RT-qPCR analysis.

2.9.1 Cell proliferation analysis—To assess cell viability, we used the IncuCyte S3® system (EssenBioscience), in which the cell density and shape are observed by photonic microscopy, while cells are maintained under standard culture conditions. UACC-62 control and siRNA treated cells were seeded in a 6-well plate. Real-time live-cell images were taken every 2 hours. To analyze cell viability, confluence was automatically calculated for 5 days, using the Basic Analyzer segmentation mask of the IncuCyte software 2019B.

2.9.2 Cell viability assays—UACC-62 were seeded in 96-well plates and treated with the control and CT55 siRNAs for 1, 3 or 5 days in triplicate, before ATP assessment with

the ATPlite 1-step kit (PerkinElmer, Waltham, MA, USA). Cell viability was analyzed by Crystal Violet staining. After 5 days, cells were fixed with 4% paraformaldehyde (Thermo Fisher Scientific, Cat.# FB002) for 15 min at room temperature. Cells were rinsed twice with PBS, stained with Crystal Violet 0.1% (Sigma, Ref.# C0775–25G) for 10 min at room temperature and washed 3 times with distilled water. Then, acetic acid 10% was added and incubated for 20 min under agitation at room temperature. Absorbance was measured using a microplate reader at 590 nm (CLARIOstar®, BMG Labtech).

3. Results

3.1 CT55 is co-expressed with other CTAs, and is associated with poor survival prognosis

We first investigated the link between CT55 expression and patient prognosis, using the NCI Genomic Data Commons (GDC) database, which contains the largest and most comprehensive cancer genomic datasets as The Cancer Genome Atlas (TCGA) and Therapeutically Applicable Research to Generate Effective Therapies (TARGET) [15]. We found that patients with tumors expressing wild-type (WT) CT55 were associated to poorer survival compared to patients with tumors expressing mutated CT55 (585 patients with WT CT55 versus 71 patients with mutated CT55, Fig. 1A, Table S1). Same result was obtained when patients with tumors expressing WT CT55 were compared to all patients with tumors also not expressing CT55 (Fig. S1). Moreover, the difference in survival rates was further enhanced when we limited our analysis to patients with tumors expressing deleterious CT55 mutations (26 patients). Finally, to investigate whether CT55 expression was correlated to the expression of others CTAs in several types of cancers, as observed in head and neck squamous cell carcinoma [11], we used the NCI60 database containing the transcriptome data of 60 cancer cell lines from 9 different tissues. Interestingly, we found that among the 561 genes correlated to CT55 mRNA expression, 51 belong to the CTA family, (CTDatabase, http://www.cta.lncc.br/), including 10 from the MAGEA family, MAGEA1, 2, 3, 4, 5, 6, 8, 10 and 12 (Fig. 1B). Taken together, these results show that CT55 is often co-expressed with other CTAs and that its expression in cancer tissues is associated with poor prognosis in patients.

3.2 CT55 is required for cell proliferation

As CT55 expression worsens patient prognosis, we investigated whether it affects cell proliferation. Cell density and shape in the presence or absence of CT55 were assessed using the IncuCyte S3 system in standard culture conditions. Efficient CT55 silencing (Fig. S2) drastically reduced cell proliferation after 3 and 5 days (Fig. 2A). This result was confirmed by crystal violet staining, showing a 50% reduction in cell proliferation after inhibition of CT55 expression during 5 days (Fig. 2B). Finally, assessment of ATP levels, as a marker of cell proliferation, disclosed a drastic reduction after SiCT55 treatment, correlating with the inhibition of cell proliferation (Fig. 2C).

To gain further insights in the molecular process leading to the inhibition of cell proliferation associated to CT55 silencing, we performed RNA-seq analysis of UACC-62 cells treated for 3 days with control siRNAs or with SiCT55. First, transcriptome analysis confirmed

the clear decrease of CT55 mRNA by the SiCT55 treatment, while its expression remained high in SiCtrl cells (Table S2). Principal component analysis of RNA-seq data revealed a significant difference (PC1 = 57%) between cells treated with SiCT55 and control cells (untreated and SiCtrl-treated cells, Fig. 2D). We identified 429 up-regulated genes and 1140 down-regulated genes in CT55 silenced cells compared to those control cells (Fig. 2E). Analysis of the up-regulated genes using gene ontology did not reveal significant altered pathways. In contrast, analysis of the 1140 down-regulated genes mainly revealed two altered pathways, cell division/proliferation, strengthening our previous results, and DNA replication (Fig. 2F). This was further confirmed by RT-qPCR mRNA quantification of PCNA, MKi67 and TOP2A, three of those 1140 genes involved in cell proliferation and DNA replication (Fig. 2G). Altogether, these results indicate that CT55 is required for cancer cell proliferation.

3.3 CT55 is localized to mitochondria and endoplasmic reticulum

Given the fact that cancer cell proliferation is influenced by mitochondrial functions [19] and CT55 is predicted to be targeted to mitochondria, we first analyzed its localization within the cell. First, using a new tool, Deeploc-1.0 [20], we found that among the 147 mitoCTAs transcripts, CT55 shows the highest predicted score (0.941 out of 1, Fig. S3A). Similarly, the InterPro analysis of CT55 primary sequence disclosed a potential N-terminus mitochondrial targeting signal (MTS), consisting of 12 amino-acids positively charged and predicted to adopt an α-helix secondary structure by I-TASSER (Fig. S3B and C). We thus investigated the role of the 12aa N-terminus sequence in the cellular localization of CT55a. We generated a collection of GFP-tagged protein constructs and assessed their localization by live cell fluorescence confocal microscopy. Our images show that GFP alone presents a diffused localization throughout the cell (Fig. 3A, A'). In contrast, CT55a co-localizes with the mitochondria, as well as the endoplasmic reticulum (ER) (Fig. 3B, B' and enlarged views). Strikingly, the predicted MTS sequence consisting of the N-terminus 12 aa of CT55, localizes exclusively to the mitochondria confirming the *in silico* analysis (Fig. 3C). This suggests that an additional localization signal may be present elsewhere in CT55a sequence, leading to its dual-localization in both organelles. In this respect, hydrophobicity analysis of CT55 primary sequence revealed two distinct domains at the N-terminus: the 12 aa MTS followed by a very hydrophilic domain, from amino-acid 13 to 30 (Fig. S3D). Therefore, we investigated the GFP localization driven by the first 30 aa N-terminus sequence. We found GFP localized in both mitochondria and ER, indicating that the 15 to 30 N-terminus hydrophilic sequence is required for ER localization (Fig. 3D, Fig. S3E). Finally, CT55 deleted for the first 30 aa (CT55Δ30aa), shows a similar pattern as GFP alone (Fig. 3E). Altogether, these results indicate that CT55 harbors a N-terminal "ambiguous" targeting signal leading to its dual localization to ER and mitochondria.

3.4 CT55 controls mitochondrial DNA replication

As we show that CT55 is localized in the mitochondria and we revealed the decrease in genes involved in DNA replication with RNAseq analysis, we investigate whether CT55 could impact mtDNA maintenance. We first assessed the link between CT55 protein levels and mtDNA levels in 4 cell lines, selected from NCI60 based on their CT55 expression (Fig. S4). Western blotting confirmed that the CT55 protein levels correlates with their

transcript levels in four different cell lines: UACC-62 and SK-MEL2 that express high levels of CT55, as well as HCT-116 and SNB-75 that do not express CT55 (Fig. S4). The two isoforms CT55a and CT55b were detected in both UACC-62 and SK-MEL-2 (Fig. 4A, bottom panel). In parallel, mtDNA quantification revealed significantly higher mtDNA copy number in UACC-62 and SK-MEL-2, compared to HCT-116 and SNB-75, thus establishing a correlation between CT55 protein expression level and mtDNA copy number (Fig. 4A).

To gain further insights in CT55 functions, we focused on the UACC-62 melanoma cancer cell line, which displays the highest CT55 expression level. We first measured mtDNA copy number following CT55 silencing using a specific siRNA (SiCT55), which induced extensive depletion of both CT55 isoforms (Fig. 4B, bottom panel), coupled with a 30% decrease in mtDNA copy number, compared to cells treated with the control siRNA (SiCtrl, Fig. 4B, top panel). Furthermore, we tested whether cells lacking CT55 were defective in mtDNA replication. To this end, mtDNA of UACC-62 cells was depleted with ethidium bromide (EtBr) treatment, and the cells were then released in EtBr-free media, allowing their mtDNA levels to recover. This showed that the process was significantly slower in cells lacking CT55, compared to untreated and SiCtrl treated cells (Fig. 4C). Indeed, mtDNA copy number in control cells recovered completely to the untreated level within 5 days, while cells depleted for CT55 regained only half of the mtDNA after 5 days of recovery, thus suggesting that CT55 facilitates mtDNA replication in UACC62 cell line. We then assessed mtDNA integrity by NGS sequencing and analyzed the data using the eKLIPse tool [21]. Regardless of the presence or absence of CT55, NGS analysis did not reveal any mtDNA rearrangements or deletions (Fig. S5A).

Next, as CTAs expression is regulated by DNA methylation, we treated HCT-116 cell line, cell line not expressing CT55, with demethylating agent, 5-aza-2’-deoxycetidine, at 2,5 μM and 5 μM for three days to induce the expression of CT55. As expected, this treatment increased CT55 expression by 60 times compared to untreated cells. Strikingly, this overexpression of CT55 led to an increase in mtDNA copy number by 2 folds (Fig. 4D). Correlation analysis of mtDNA copy number and transcriptomics data in NCI60 cell lines revealed that after the secretory protein TNF Alpha Induced Protein 6 (TNFAIP6), the second highest positively correlated gene is *CT55* (Fig. 4E), indicating that its impact on mtDNA copy number is not restricted to melanoma cells (UACC-62 and SK-MEL2). Finally, although no change in the mitochondrial network structure was detected after CT55 silencing (Fig. S5B), mitochondrial respiration was much lower in cell treated with SiCT55 compared to SiCtrl (Fig. S5C). Altogether, these data show that CT55 is required for mtDNA replication in UACC-62 and its expression is correlated to mtDNA copy number in NCI60.

In conclusion, our study identified CT55, as a mitochondrial and ER protein, whose impact on mtDNA replication and proliferation in cancer cells might underlie its poor prognosis influence in cancer patients.

4. Discussion

To gain insight into the CT55 functions in mitochondrial physiology, we first examined its cell localization by analyzing its primary protein sequence, and disclosed that it includes a predicted mitochondrial targeting sequence at its N-terminus [9]. Surprisingly, the CT55-GFP fusion protein localizes to mitochondria and the ER, due to an ambiguous peptide sequence corresponding to the first 30 aa, with the first 12 aa involved in mitochondrial targeting and the next 18 aa involved in ER localization. This characterization of dual localization has been reported for other proteins [22,23]. The dual localization of CT55 suggests its possible involvement in the ER-Mitochondrial-Associated Membranes (MAMs), which are structures involved in coupling mtDNA replication to mitochondrial network fission [24]. As no change in the mitochondrial network structure was detected after CT55 silencing, we conclude that CT55 is not involved in the regulation of mitochondrial fission/fusion balance. Thus, the identification of CT55 partners should help to elucidate how CT55 links MAMs to the control of mitochondrial genome maintenance.

Functionally, we found that CT55 is important for cell proliferation, as down-regulation of CT55 is coupled with down-regulation of many genes involved in cell cycle and DNA replication, such as PCNA, MKi67 and TOP2A. These results strongly suggest that in cancer cells, CT55 couples mtDNA replication to a signaling process that regulates the hundreds of genes required for cell proliferation. By correlating the mtDNA levels to the 22.000 mRNA levels, we identified *CT55* as the second most positively correlated gene, while genes encoding the mtDNA replisome [25] (TFAM, POLG, SSBP1 and TWNK) or genes involved in mitochondrial biogenesis [26] (PGC-1α, NRF1 and NRF2) did not correlate with the mtDNA copy number. This suggests that in cancer cell lines, regulation of mtDNA levels is not directly linked to the levels of the mtDNA replisome enzymes. Using cell lines depleted for CT55, our study confirmed the pivotal role of CT55 as a potential positive regulator for mtDNA replication in cancer cells. In tumorigenesis, drastic quantitative changes in mtDNA copy number were observed in cancer cells. Certain types of cancers tend to show significant mtDNA reduction, such as bladder and breast cancers [27], kidney and hepatocellular carcinoma [28] and myeloproliferative neoplasm [29], while other types of cancers tend to associate with increased mtDNA levels, including chronic lymphocytic leukemia, lung squamous cell carcinoma and pancreatic adenocarcinoma [29]. These observations demonstrate that mtDNA levels are tightly regulated according to the cancer type. Our study shows that CT55 might serve as a major contributor in this complex process. Therefore, understanding how CT55 regulates mtDNA levels will have important ramifications, as high levels of CT55 expression in cancer tissues are linked to poor prognosis in patients. Thus, elucidating the precise molecular mechanism of CT55-mediated cell proliferation might lead to potential development of new cancer therapy. *CT55* belongs to the *CTA* gene family, which has a highly peculiar expression pattern as it is restricted to gametogenesis and cancer cells. The data presented here potentially shed light on the specific role of CT55 during spermatogenesis, as a physiological contributor, and during tumorigenesis, as a pathological contributor. It is well known that in both processes, drastic variations of mtDNA copy number are observed. During the early stages of spermatogenesis, mtDNA replication must be promoted in order to support the energy requirement of active

cell proliferation. However, during the spermatozoon maturation process, mtDNA level must decrease from hundreds of copies to very few copies to prevent paternal mtDNA transmission [30,31] and to promote fertility [32]. Thus, it is possible that *CT55* expression is high during the early proliferation phases of spermatogenesis, before its expression is switched off during the maturation process, in order to decrease mtDNA levels.

Finally, we observed that CT55 is co-expressed with 51 other CTAs, among which 14 belong to the MAGE family. Importantly, it is well documented that CTA co-expression is associated with cancers with poor prognosis, because they promote resistance to chemotherapeutic drugs, inhibition of apoptosis and ultimately cell proliferation [33]. For instance, multiple myeloma patients expressing more than 6 CTAs have a much poorer prognosis than those expressing less than 6 CTAs [3]. Therefore, the level of CT55 might serve as indicator of pathological prognosis. Indeed, patients with tumors expressing inactive CT55 survive longer than patients expressing wild-type CT55. Altogether, we demonstrate here that CT55 is involved in mtDNA maintenance and cell proliferation, and thus CT55 could potentially serve as a valid therapeutic target for cancer therapy.

Supplementary Material

Refer to Web version on PubMed Central for supplementary material.

Funding

This work was supported by the Université d'Angers, CHU d'Angers, the Région Pays de la Loire and Angers Loire Métropole, PULSAR. This study supported by the Center for Cancer Research, the intramural program of the National Cancer Institute (BC 006150).

References

1. van der Bruggen P et al. A gene encoding an antigen recognized by cytolytic T lymphocytes on a human melanoma. Science 254, 1643–1647 (1991). [PubMed: 1840703]
2. Almeida LG et al. CTdatabase: a knowledge-base of high-throughput and curated data on cancer-testis antigens. Nucleic Acids Res. 37, D816–D819 (2009). [PubMed: 18838390]
3. Andrade VCC et al. Prognostic impact of cancer/testis antigen expression in advanced stage multiple myeloma patients. Cancer Immun. J. Acad. Cancer Immunol. 8, (2008).
4. Hüttemann M, Jaradat S & Grossman LI Cytochrome *c* oxidase of mammals contains a testes-specific isoform of subunit VIb-the counterpart to testes-specific cytochrome *c*?: COX VIb TESTES. Mol. Reprod. Dev. 66, 8–16 (2003). [PubMed: 12874793]
5. Cheng C-C et al. Sperm-specific COX6B2 enhances oxidative phosphorylation, proliferation, and survival in human lung adenocarcinoma. eLife 9, e58108 (2020). [PubMed: 32990599]
6. Nie K et al. COX6B2 drives metabolic reprogramming toward oxidative phosphorylation to promote metastasis in pancreatic ductal cancer cells. Oncogenesis 9, 51 (2020). [PubMed: 32415061]
7. Doghman-Bouguerra M et al. FATE1 antagonizes calcium- and drug-induced apoptosis by uncoupling ER and mitochondria. EMBO Rep. 17, 1264–1280 (2016). [PubMed: 27402544]
8. Maxfield KE et al. Comprehensive functional characterization of cancer-testis antigens defines obligate participation in multiple hallmarks of cancer. Nat. Commun. 6, 8840 (2015). [PubMed: 26567849]
9. Aurrière J et al. Cancer/Testis Antigens into mitochondria: a hub between spermatogenesis, tumorigenesis and mitochondrial physiology adaptation. Mitochondrion 56, 73–81 (2021). [PubMed: 33220498]

10. Dong X-Y, Li Y-Y, Yang X-A & Chen W-F BJ-HCC-20, a potential novel cancer-testis antigen. Biochem. Cell Biol. 82, 577–582 (2004). [PubMed: 15499386]
11. Zamuner FT et al. A Comprehensive Expression Analysis of Cancer Testis Antigens in Head and Neck Squamous Cell Carcinoma Revels MAGEA3/6 as a Marker for Recurrence. Mol. Cancer Ther. 14, 828–834 (2015). [PubMed: 25564441]
12. Matsushita M et al. CXorf48 is a potential therapeutic target for achieving treatment-free remission in CML patients. Blood Cancer J. 7, e601–e601 (2017). [PubMed: 28862699]
13. Zhao H et al. Cancer testis antigen 55 deficiency attenuates colitis-associated colorectal cancer by inhibiting NF-κB signaling. Cell Death Dis. 10, 304 (2019). [PubMed: 30944312]
14. Zong W-X, Rabinowitz JD & White E Mitochondria and Cancer. Mol. Cell 61, 667–676 (2016). [PubMed: 26942671]
15. Grossman RL et al. Toward a Shared Vision for Cancer Genomic Data. N. Engl. J. Med. 375, 1109–1112 (2016). [PubMed: 27653561]
16. McLaren W et al. The Ensembl Variant Effect Predictor. Genome Biol. 17, 122 (2016). [PubMed: 27268795]
17. Ng PC SIFT: predicting amino acid changes that affect protein function. Nucleic Acids Res. 31, 3812–3814 (2003). [PubMed: 12824425]
18. The Gene Ontology Consortium. The Gene Ontology Resource: 20 years and still GOing strong. Nucleic Acids Res. 47, D330–D338 (2019). [PubMed: 30395331]
19. Boyle KA et al. Mitochondria-targeted drugs stimulate mitophagy and abrogate colon cancer cell proliferation. J. Biol. Chem. 293, 14891–14904 (2018). [PubMed: 30087121]
20. Almagro Armenteros JJ, Sønderby CK, Sønderby SK, Nielsen H & Winther ODeepLoc: prediction of protein subcellular localization using deep learning. Bioinformatics 33, 3387–3395 (2017). [PubMed: 29036616]
21. Goudenège D et al. eKLIPse: a sensitive tool for the detection and quantification of mitochondrial DNA deletions from next-generation sequencing data. Genet. Med. 21, 1407–1416 (2019). [PubMed: 30393377]
22. Yogev O & Pines O Dual targeting of mitochondrial proteins: Mechanism, regulation and function. Biochim. Biophys. Acta BBA - Biomembr. 1808, 1012–1020 (2011).
23. Bodył A & Mackiewicz P Analysis of the targeting sequences of an iron-containing superoxide dismutase (SOD) of the dinoflagellate Lingulodinium polyedrum suggests function in multiple cellular compartments. Arch. Microbiol. 187, 281–296 (2007). [PubMed: 17143625]
24. Lewis SC, Uchiyama LF & Nunnari J ER-mitochondria contacts couple mtDNA synthesis with mitochondrial division in human cells. Science 353, aaf5549 (2016). [PubMed: 27418514]
25. Korhonen JA, Pham XH, Pellegrini M & Falkenberg M Reconstitution of a minimal mtDNA replisome in vitro. EMBO J. 23, 2423–2429 (2004). [PubMed: 15167897]
26. Wu Z et al. Mechanisms Controlling Mitochondrial Biogenesis and Respiration through the Thermogenic Coactivator PGC-1. Cell 98, 115–124 (1999). [PubMed: 10412986]
27. Castellani CA, Longchamps RJ, Sun J, Guallar E & Arking DE Thinking outside the nucleus: Mitochondrial DNA copy number in health and disease. Mitochondrion 53, 214–223 (2020). [PubMed: 32544465]
28. Reznik E et al. Mitochondrial DNA copy number variation across human cancers. eLife 5, e10769 (2016). [PubMed: 26901439]
29. Consortium PCAWG et al. Comprehensive molecular characterization of mitochondrial genomes in human cancers. Nat. Genet. 52, 342–352 (2020). [PubMed: 32024997]
30. Rantanen A & Larsson NG Regulation of mitochondrial DNA copy number during spermatogenesis. Hum. Reprod. Oxf. Engl. 15 Suppl 2, 86–91 (2000).
31. DeLuca SZ & O'Farrell PH Barriers to Male Transmission of Mitochondrial DNA in Sperm Development. Dev. Cell 22, 660–668 (2012). [PubMed: 22421049]
32. May-Panloup P et al. Increased sperm mitochondrial DNA content in male infertility. Hum. Reprod. Oxf. Engl. 18, 550–556 (2003).
33. Fratta E et al. The biology of cancer testis antigens: putative function, regulation and therapeutic potential. Mol. Oncol. 5, 164–182 (2011). [PubMed: 21376678]

34. Yang J et al. The I-TASSER Suite: protein structure and function prediction. Nat. Methods 12, 7–8 (2015). [PubMed: 25549265]

Highlights

Cancer/Testis Antigens 55 (CT55) expression in cancer is associated with poor survival and Its silencing decreases dramatically cancer cell proliferation.

CT55 is localized to both mitochondria and endoplasmic reticulum (ER) due to the presence of an ambiguous N-terminal targeting signal.

CT55 silencing decreases mtDNA copy number and delays mtDNA recovery after an acute depletion. Finally, CT55 expression is strongly correlated to mtDNA amount in NCI-60 cell lines.

Summary Statement:

CT55 is localized to mitochondria and endoplasmic reticulum and is correlated to mtDNA copy number across NCI-60. Its silencing decreases mtDNA amount and cell proliferation. Tumors expressing CT55 are associated with a poor prognosis.

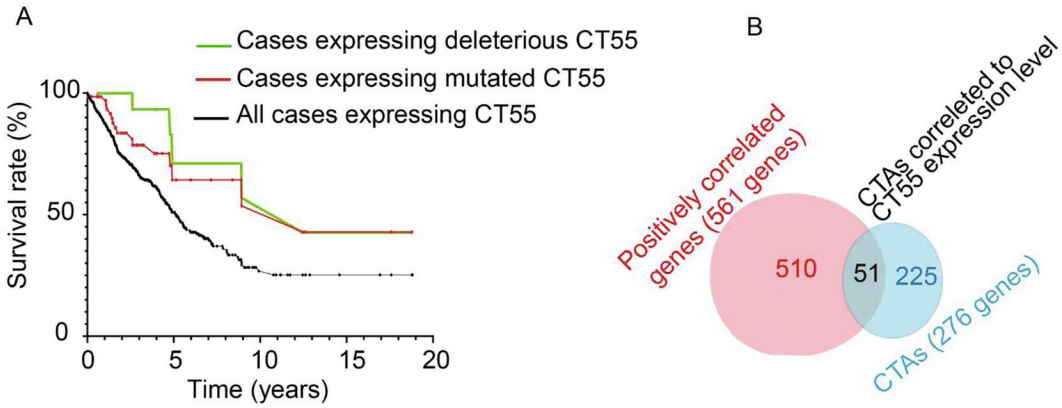

Figure 1: CT55 expression is linked to the poor prognosis of patients with cancer.

A) NCI Genomic Data Commons (GDC) analysis showing the survival data of cases with tumors expressing CT55 (585 cases, black line), cases expressing mutated CT55 based on Ensembl Variant Effect Predictor (VEP) [16] impact (71 cases, red line) and cases expressing deleterious mutated CT55 based on a deleterious Sorting Intolerant From Tolerant (SIFT) [17] impact (26 cases, green line). **B)** Co-expression of CT55 with other CTAs. Among the 561 positively correlated genes with CT55 in NCI-60 cell lines, 51 belong to the CTA database.

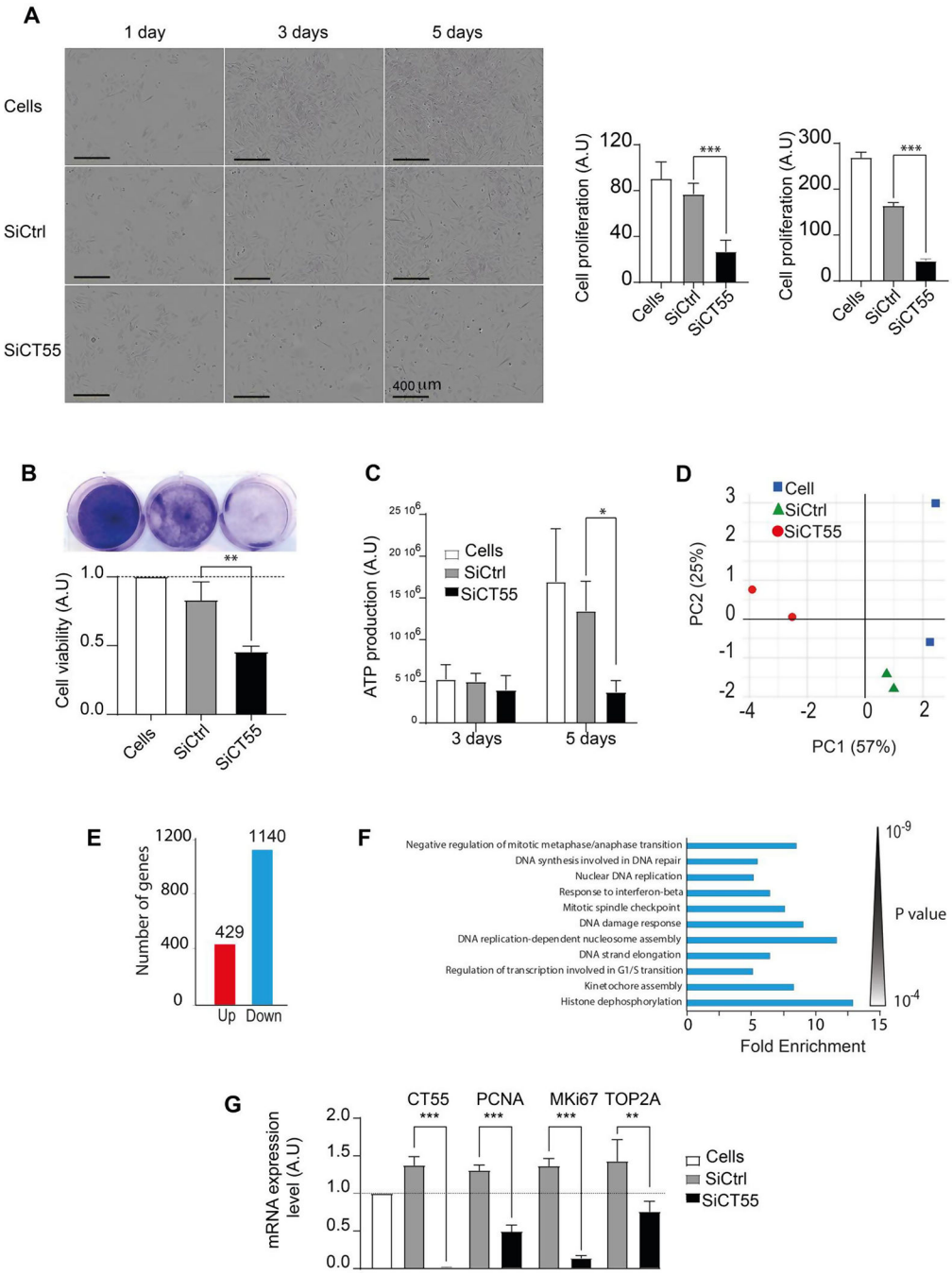

Figure 2: CT55 sustains cell proliferation:

A) Left panels: representative real time images, of UACC-62 control cells (top), or treated with the control (middle) and CT55 (bottom) siRNA for 1, 3 and 5 days, Scale barre = 400 µm. Right panels show the confluence quantifications. **B)** Upper panels: representative images of crystal violet staining of control and siRNA treated cells after 5 days; and lower panels show the staining quantification (n=6). **C)** Measurements of the ATP production using the ATPLite assay (n=3). **D)** Principal component analysis (PCA) of the RNA-seq data shows one cluster including the UACC-62 untreated cells (bleu) and SiCtrl (green) on the

right and CT55 silenced cells (red), on the left. **E)** Total number of genes up (red) or down (blue) regulated with a fold change >2 between control cells (untreated + SiCtrl) and CT55 silenced cells. **F)** PANTHER gene ontology[18] of enriched pathways including the 1158 downregulated genes. **G)** RT-qPCR mRNA expression level of PCNA, MKi67 and TOP2A genes involved in cell proliferation. M±SEM (n=3), *: P<0,05; **: P<0,01; ***: P<0,001. Mann-Whitney test.

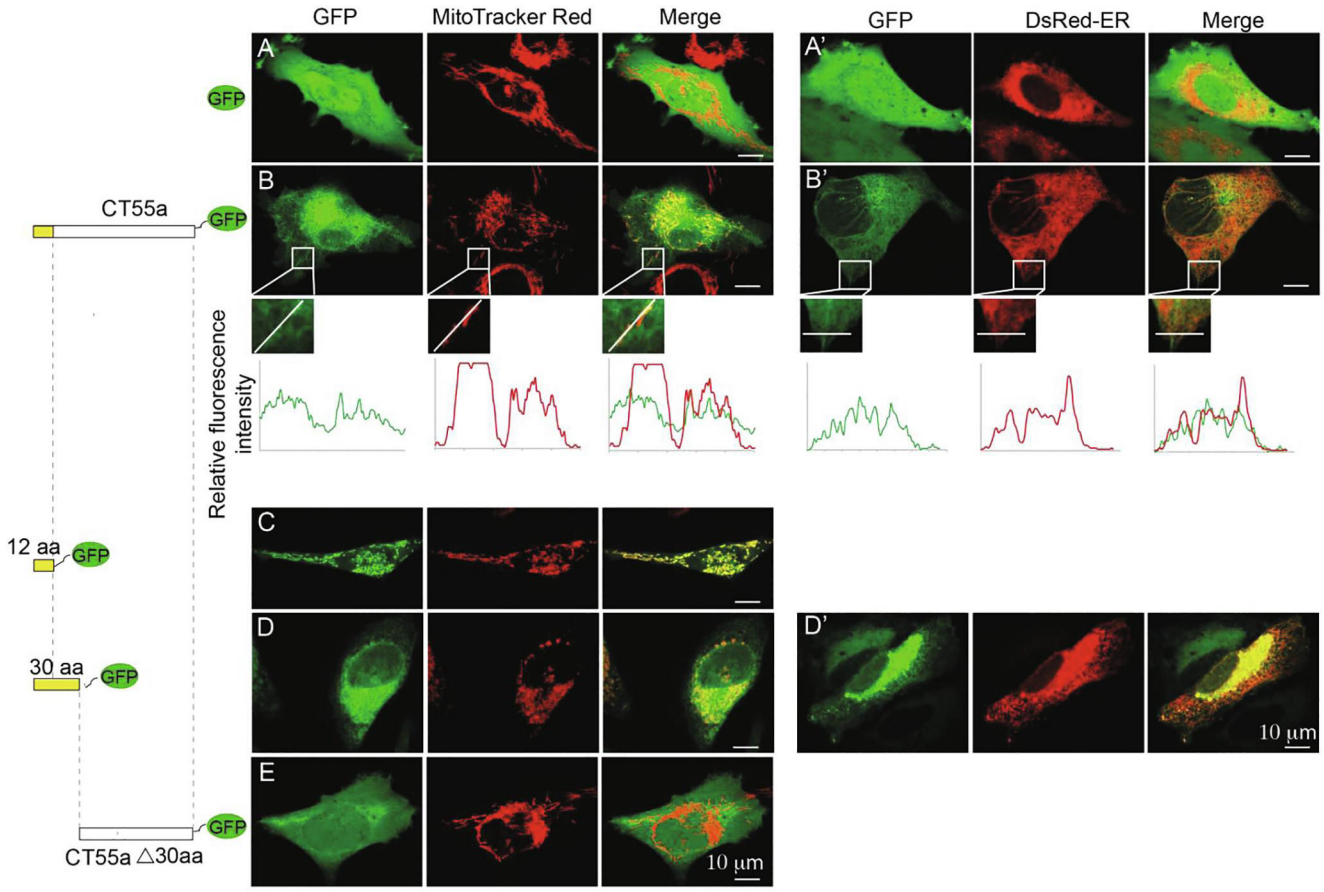

Figure 3: CT55 localizes to mitochondria and ER.

Fluorescence microscopy images of UACC-62 cells transfected with the indicated CT55a constructs (as represented at left of each panel) tagged at C-terminal end with a GFP. A, B, C, D and E) Columns from left to right show GFP (green), MitoTracker Red for mitochondrial staining (red), and merged images. A', B' and D') Columns from left to right show GFP (green), DsRed-ER for ER staining (red) and merged images. B and B') Enlarged views of the inset areas show the co-localization of the green and red staining. Lines drawn in the enlarged views show the relative fluorescence intensity of the red and green staining.

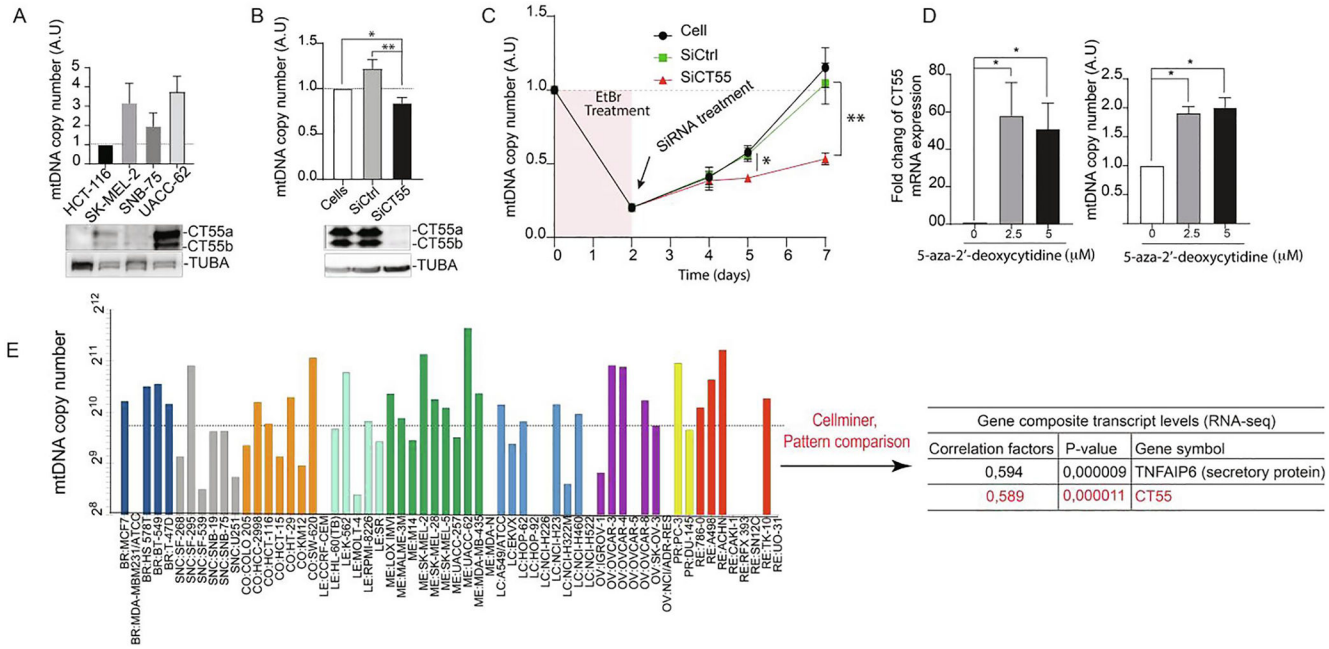

Gene composite transcript levels (RNA-seq)		
Correlation factors	P-value	Gene symbol
0,594	0,000009	TNFAIP6 (secretory protein)
0,589	0,000011	CT55

Figure 4: CT55 controls mtDNA copy number.

A) top panel: mtDNA copy number in HCT-116, SK-MEL-2, SNB-75 and UACC-62 cell lines; bottom panel: Western blot showing the expression level of CT55 isoforms in these four cell lines (n=4). **B)** Top panel: mtDNA copy number in untreated UACC-62 and after treatment with the control (SiCtrl) and CT55 (SiCT55) siRNAs for 5 days. Bottom panel: Western blot showing the expression level of the two CT55 isoforms before and after siRNA treatment (n=6). **C)** mtDNA depletion and recovery in UACC-62 cells. Cells were treated with 200 nM of EtBr for 2 days, then released while simultaneously treated with the indicated siRNA in absence of EtBr. mtDNA copy number was quantified at the indicated days (n=4). * P<0,05; ** P<0,01. Test Mann-Whitney (B). Test ANOVA (C). **D)** mRNA expression levels of CT55 and PDK2 in the same four cell lines. *PDK2* mRNA expression is the highest negatively correlated gene to CT55 expression level across NCI-60 database. **D)** CT55 mRNA expression and mtDNA copy number of untreated and treated HCT-116 cell line with 5-aza-2'-dexoycyditine at 2,5 µM and 5 µM for 3 days. **E)** Quantification of mtDNA copy number in the NCI-60 cell lines. CellMiner pattern comparison identified CT55 as the second highest positively correlated gene with mtDNA copy number.